A Quasi-Optical Free-Space Measurement Setup Without Time-Domain Gating for Material Characterization in the W-Band

Daniel Bourreau, Alain Péden, and Sandrick Le Maguer

***Abstract*—In this paper, a new free-space measurement setup at millimeter waves for material characterization is presented. Using specific Gaussian optics lens antennas and a thru, reflect, and line calibration, the setup provides the free-space four S-parameters over the W-band of planar dielectric slabs without time-domain gating. An efficient optimization procedure is implemented to extract complex permittivity from the four S-parameters of homogeneous dielectric materials. Nonhomogeneous materials can also be tested, and measurements are presented. Very good agreement is observed between simulated and measured four S-parameters of various dielectric plates. Thanks to this new specific calibration and measurement procedure, automation of the test bench is easily achieved.**

***Index Terms*—Free-space calibration, free-space setup, Gaussian beam, material characterization, permittivity measurement.**

I. Introduction

THE RELATIVE permittivity is an important electrical property of dielectric materials such as substrates, radomes, lens antenna, etc. Its value must be accurately known to perform the design of microwave and millimeter wave circuits. Many techniques are available for the characterization of this parameter at high frequencies [1]. The first class of characterization techniques requires rectangular or coaxial waveguides or cavities where machined samples are inserted [2]. The major drawback of the waveguide approach in the millimeter wave range is that the waveguide dimensions decrease. As a consequence, the sample material size becomes a critical parameter since its machining tends to be difficult. On the other hand, resonant methods that use cavities are known to provide high accuracy measurement for low-loss materials but are limited to a single frequency [3]. Regarding these drawbacks, a second class of techniques seems very attractive: free-space (or quasi-optical) methods [4]. They do not require specific and accurate sample machining and hence are contactless and nondestructive. Furthermore, broadband characterization can be achieved.

The free-space technique is therefore an interesting solution especially in the W-band: The sample preparation is easy, and the technique is suitable for a large range of materials. A planar dielectric slab or material is inserted into a free-space transmission path between two horn-lens antennas; and the permittivity extraction is based on the four S-parameter measurements or only on reflection or transmission coefficient measurements at different polarization states and/or incidence angles. Some of the results presented are at a single frequency or over a wide frequency range because broadband capabilities of this kind of test bench mainly depend on the antenna design [5]–[10]. Furthermore, the implementation of such a bench must avoid diffraction effects at the edges of the sample. Thus, spot-focusing horn-lens antennas for minimizing this phenomenon are often preferred [11].

The new free-space test bench presented in this paper performs characterization in the W-band using spot-focusing antennas. Moreover, to achieve an efficient extraction of relative permittivity, a new technique is used to ensure plane-wave assumption through the whole sample: horn-lens antennas that were designed for paraxial beam radiating are used [12]. This is a major feature in our procedure because the plane-wave assumption with Gaussian distribution of the transverse electromagnetic field is a very good approximation while the energy is concentrated around the propagation axis [13]. Incidentally, this approach has the advantage of not requiring any absorbing material around the horn-antennas and the sample holder.

To ensure accurate extraction of the material permittivity, calibration of the test bench is performed. In the present approach, a free-space thru, reflect, line (TRL) calibration is developed without time gating. Note that time gating is the usual processing to eliminate the standing waves and errors due to multiple reflections [14]. Eliminating this step leads to a robust calibration: readjusting of the time bandpass filter to accommodate each material is avoided. A specific procedure is also applied to avoid position errors because neither the antennas nor the carrier of the circuit is moved after calibration. The reference planes are therefore well known. These features are major advantages since a straightforward automation of the bench is now possible.

Moreover, a new systematic verification of the characterization is presented. This technique is based on the comparison of the measured and calculated four S-parameters: the permittivity is determined using the transmission coefficient S_{21} while the two reflection coefficients S_{11} and S_{22} are used for verification. This comparison also enables refining the value of the slab thickness.

Manuscript received February 22, 2005; revised August 23, 2006.

The authors are with the Laboratoire d'Electronique et des Systèmes de Télécommunications (LEST), Ecole Nationale Supérieure des Télécommunications de Bretagne, Unité Mixte de Recherche (UMR 6165), Centre National de la Recherche Scientifique (CNRS), 29238 Brest Cedex 3, France (e-mail: Alain.Peden@enst-bretagne.fr).

Digital Object Identifier 10.1109/TIM.2006.884283

0018-9456/$20.00 © 2006 IEEE

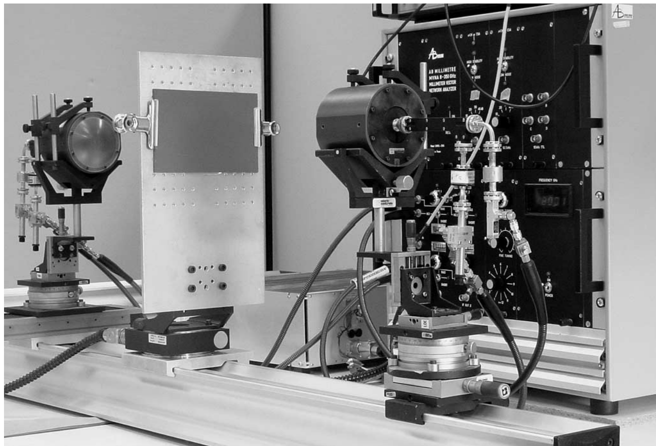

Fig. 1. Test bench in the W-band composed of two Gaussian beam horn antennas facing each other. Material sample is being measured.

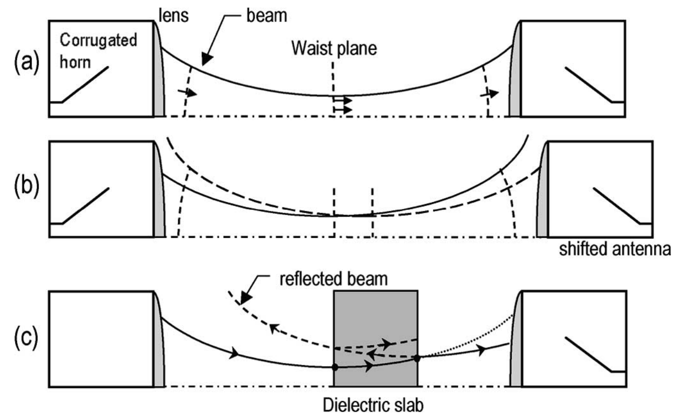

Fig. 2. Problems encountered with a focused Gaussian beam test bench. (a) Waist position between the focusing horns. (b) Beam growth when one of the antennas is shifted. (c) Spurious reflection of the beam when a slab is inserted. Note that for convenience, only half of the beam and horns is represented.

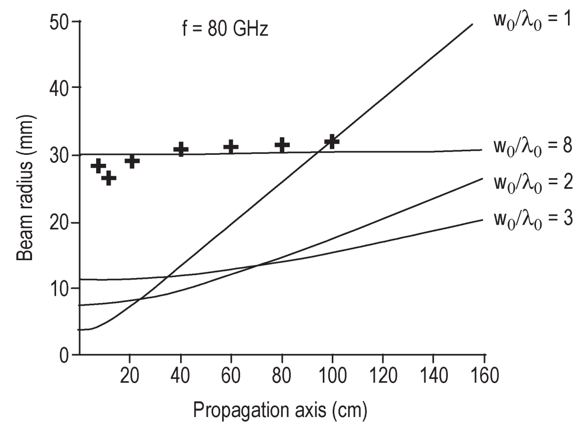

Fig. 3. Gaussian beam radius variation along the propagation axis. Measured data (crosses) from GOLA antennas used in the test bench represented in Fig. 1 and compared with various theoretical evolutions (continuous lines).

Finally, some experimental results are provided for various materials which validate the test bench and the associated extraction procedures.

II. Measurement Setup Description

The measurement setup developed is shown in Fig. 1. It is composed of two purchased Gaussian beam horns [Gaussian optics lens antennas (GOLAs)], a sample holder and an ABmm millimeter vector network analyzer [15] controlled by a computer. The antennas and the sample holder are mounted on a rail to achieve accurate alignment of the sample into the antenna beam. Furthermore, positioners are used to control position with a precision of 10 μm in the three directions of the Cartesian space. The distance between the horns is about 60 cm, which affords a very compact bench.

A. Focused Gaussian Beam Theory

When using a free-space characterization technique, antenna beam growth is a major drawback to achieve energy concentration on the dielectric slab. To avoid such a phenomenon, a dielectric lens can be used to refocus the beam [12]. Consequently, a focusing horn has to be made up of a corrugated horn and a lens. The corrugated horn produces a Gaussian beam that is focused by the dielectric lens [16], [17]. In the focal plane of the beam [i.e., waist plane, see Fig. 2(a)], the longitudinal component of the electric field does not exist, so that a dielectric slab can be placed there for characterization under the plane-wave assumption which simplifies relative permittivity extraction. In the same manner, most of the beam waist energy should be intercepted by the plate with the result that its transverse size must be large enough to reduce diffraction effects on the edges of the slab. Thus, the focused beam is interesting in that it reduces this size, but one has to take into account an important drawback, which is that the focusing horns cannot focus in the same plane over a wide frequency range. Consequently, the incident wavefront on the slab has properties which depend on the frequency; moreover, the slab is not located in the unique waist plane because of its thickness [see Fig. 2(c)]. This is also a critical point when shifting one antenna away from the other [see Fig. 2(b)] during the calibration process (see Section II-B).

To overcome these drawbacks, a radiated paraxial beam should be used as a negligible variation of the beam diameter along the propagation axis is obtained. This kind of beam is based on the following principle: the electric field propagates at small angles to the propagation axis which is the basis of the paraxial approximation [13]. The smaller the waist diameter, the less paraxial the beam. The paraxiality obtained solves the problems associated with the positioning of the slabs during the measurement procedure and standards during the calibration procedure.

According to the Gaussian beam theory, the paraxiality of a beam is expressed by its w_0/λ_0 value (w_0 is the beam waist diameter and λ_0 is the wavelength in free space) [18], [19]. The greater the w_0/λ_0 ratio, the more paraxial the beam. Fig. 3 shows the theoretical beam radius variation along the propagation axis for different w_0/λ_0 values. The beam radius of the GOLA antennas mounted in the test bench is determined by measurements (see dots in Fig. 3). Thus, a w_0/λ_0 value of 8 is obtained which corresponds to a very paraxial beam. The waist diameter is around 50–60 mm at 80 GHz. Measurements

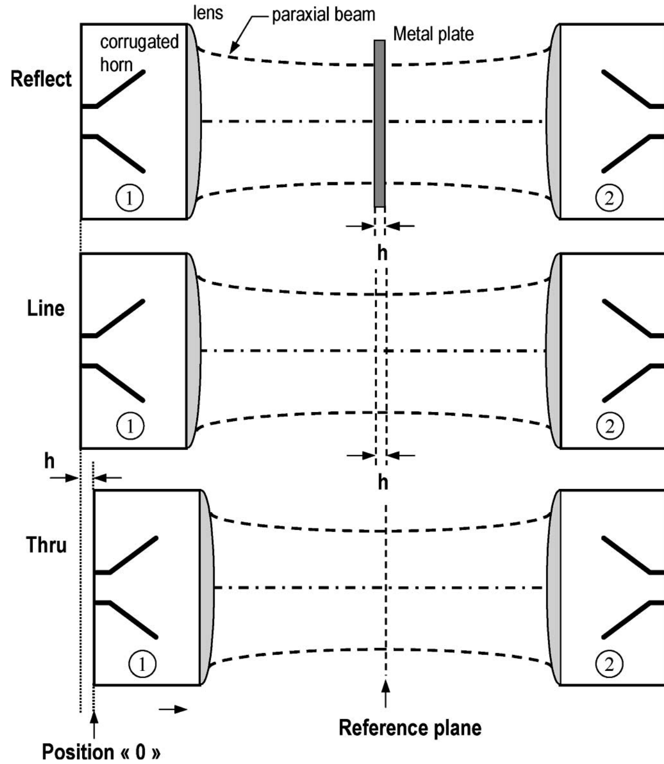

Fig. 4. Free-space TRL calibration procedure of the test bench. A metal plate is used for the Reflect standard and antenna (1) is moved back from position "0" to a distance h equal to the metal plate thickness. The Line standard is obtained by removing the metal plate and keeping the distance between the two horns unchanged. The Thru standard is achieved by moving antenna (1) back to position "0."

from 75 to 110 GHz show a narrower beam with increasing frequency. As a consequence, the sample size has to be around $10 \times 10\ \text{cm}^2$.

B. Test Bench Calibration

As the characterization of dielectric materials is based on the four S-parameter measurements using a vector network analyzer, calibration has to be performed to correct raw S-parameters. The raw S-parameters which are measured using dual directional couplers and detectors must be error-corrected to obtain the actual S-parameters at the material interfaces. Among the calibration procedures, the well-known TRL calibration technique [20] is well appropriate for free-space calibration because the three standards could be readily implemented. Furthermore, the paraxial beam used here guaranties the TRL basic assumption that there is only a single beam propagation mode and a unique Z_0 normalization impedance (free-space impedance). Moreover, the beam characteristics are nearly unmodified when one antenna is shifted (for example, when performing the line standard measurement). Finally, to minimize position errors, the following procedure for calibration is applied (see Fig. 4):

1) The Reflect standard is achieved by mounting a metal plate on the carrier and moving back antenna (1) from position "0" to a distance h equal to the thickness of the reflect metal plate.
2) The Line standard is obtained by removing the metal plate and keeping the distance between the two horns unchanged. The Line length L must verify: $10^\circ < k_0 \cdot L < 170^\circ$ over the frequency range, where $L = h$ and $k_0 = 2\pi/\lambda_0$, to avoid any phase ambiguity during the extraction of the calibration error terms.
3) The Thru standard is achieved by moving antenna (1) back to position "0."

When the calibration is completed, the reference planes of the two reflection coefficients are both located in the same plane (referred to as "reference plane" in Fig. 4). The position of the holder and antenna will never change during the measurement of the dielectric materials. Consequently, errors due to the sample positioning (phase shift, etc.) are eliminated.

III. Permittivity Extraction Procedure

The extraction of the complex relative dielectric constant ε_r of various homogeneous materials is based on the S_{21} parameter measurement. The analytical S_{11} and S_{21} parameters of an infinite planar dielectric slab under plane-wave assumption are given by the following equations [21]:

$$S_{21} = S_{12} = \frac{(1-\rho^2)\cdot\exp(-j\Gamma h)}{1-\rho^2\cdot\exp(-2j\Gamma h)} \tag{1}$$

$$S_{11} = S_{22} = \frac{\rho\cdot(1-\exp(-2j\Gamma h))}{1-\rho^2\cdot\exp(-2j\Gamma h)} \tag{2}$$

with

$$\rho = \frac{1-\sqrt{\varepsilon_\mathrm{r}}}{1+\sqrt{\varepsilon_\mathrm{r}}}, \quad \Gamma = \frac{2\pi}{\lambda_0}\cdot\sqrt{\varepsilon_\mathrm{r}}$$

and

$$\varepsilon_\mathrm{r} = \varepsilon_\mathrm{r}' + j\varepsilon_\mathrm{r}'' = \varepsilon_\mathrm{r}'(1-\tan\delta)$$

where λ_0 is the free-space wavelength, h is the slab thickness, and the loss tangent is calculated by $\tan\delta = -\varepsilon_\mathrm{r}''/\varepsilon_\mathrm{r}'$ with $\varepsilon_\mathrm{r}'' < 0$. As ε_r cannot be expressed explicitly in terms of S_{11} or S_{21} from (1) or (2), it is determined from the complex S_{21} parameter using an optimization procedure (zero finding using quasi-Newton optimization). To achieve this, a meaningful error function (EF) must be defined. A theoretical study of different EFs has led to the following definition of EF:

$$\mathrm{EF} = \tanh\left[\alpha\cdot\left|1-\frac{S_{21\mathrm{meas}}}{S_{21\mathrm{cal}}}\right|^2\right] \tag{3}$$

where $S_{21\mathrm{cal}}$ is the calculated parameter with (1), $S_{21\mathrm{meas}}$ is the measured and corrected parameter. The coefficient α is an adjustable parameter but its value is not critical in the determination of the EF minima. A typical value $\alpha = 0.1$ is convenient for all the characterized materials. Moreover, the $\tanh$ function in (3) is used to obtain a bounded result (between 0 and 1) when computing EF. An example of the variation of EF using (3) for one frequency point is depicted in Fig. 5. It can be observed that there are more than one solution for ε_r.

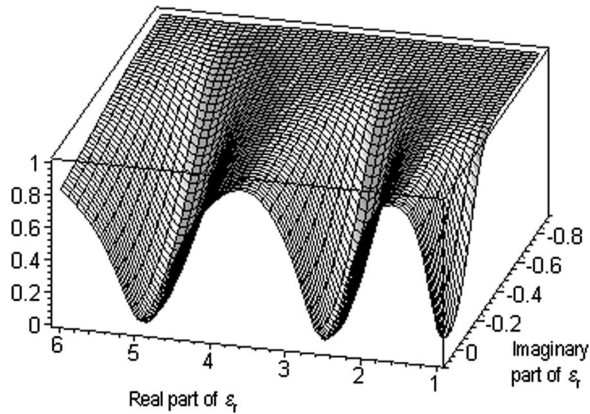

Fig. 5. 3-D EF (3) computed with $\alpha = 0.1$ for Rexolite material ($h = 12.85$ mm) at 80 GHz.

In order to obtain the actual permittivity, the following procedure is applied:

a) The three-dimensional (3-D) evolution of EF is computed varying the real part ε_r' and imaginary part ε_r'' of ε_r at one frequency point. This step provides initial estimates of ε_r' and ε_r'' which correspond to EF minima observed (see Fig. 5).

b) One of these initial estimates of ε_r is chosen and the permittivity is then extracted by means of (3) at each frequency point over the whole frequency range.

c) The calculated S-parameters at each frequency point are computed over the frequency range using the previously ε_r extracted values. The comparison between the calculated and measured four S-parameters in magnitude and phase clearly shows whether the ε_r extracted values are acceptable or not. If not, step b must be repeated using another initial value of ε_r obtained from the first step.

d) The thickness h can be precisely adjusted by comparison between the S_{11} and S_{22} calculated parameters and measurements.

Note that in c and d steps, the comparison is performed between the measured and calculated magnitudes of S_{11} and S_{22} and between the phase of the product $S_{11}S_{22}$ to overcome phase shift due to possible positioning errors of the slab during the four S-parameter measurements.

To illustrate the described procedure, Figs. 6 and 7 present the results for a dielectric slab (polyvinyl chloride (PVC), $h = 5.06$ mm). The four S-parameters are calculated with extracted values of ε_r' over the frequency band using an initial estimate of $\varepsilon_r' = 5.602$ and $\varepsilon_r'' = 0$ (minimum of EF at 80-GHz frequency point—a step). Measured and calculated S_{21} parameters are in very good agreement in Fig. 6 while large discrepancy between measured and calculated S_{11} or S_{22} coefficients is observed in Fig. 7. As previously mentioned, the phase of the product $S_{11}S_{22}$ is depicted in Fig. 7. Thus, a new initial estimate of $\varepsilon_r' = 2.9$ and $\varepsilon_r'' = 0$ (from another EF minimum) is used to extract ε_r at each frequency point (b and c steps). The simulated S-parameters are then calculated using the extracted values of ε_r. In this case, very good agreement is obtained for the four S-parameters (see Fig. 8 for S_{11} magnitude and $S_{11}S_{22}$ phase. S_{21} magnitude and phase are not shown because results are very similar to those depicted in Fig. 6). Finally, the thickness h can be precisely determined by repeating c and d steps with an initial value of $\varepsilon_r' = 2.9$ and $\varepsilon_r'' = 0$. Fig. 9 illustrates the dielectric permittivity extraction with a 5.16 mm slab thickness (100-μm difference or 2%). Fig. 9 shows a shift of the simulated resonance frequencies in the S_{11} (and S_{22}) plot while simulated and measured S_{21} parameters are very close and quite similar to results depicted in Fig. 6. Once the extraction procedure is completed, the material can exhibit a nearly constant permittivity with frequency. In this particular case, mean values of ε_r' and ε_r'' can be calculated with very low standard deviations σ. The σ values do not give the uncertainty of the measurements but indicate whether the experimental data are spread about the mean or not.

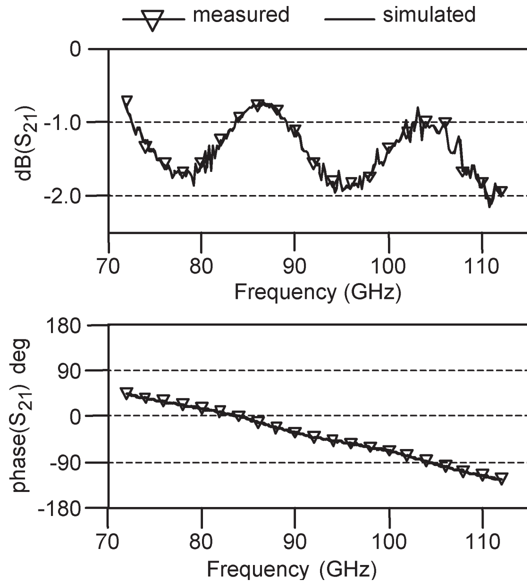

Fig. 6. Comparison between simulated and measured S_{21} parameter using an initial estimate of $\varepsilon_r' = 5.602$ from 3-D extraction.

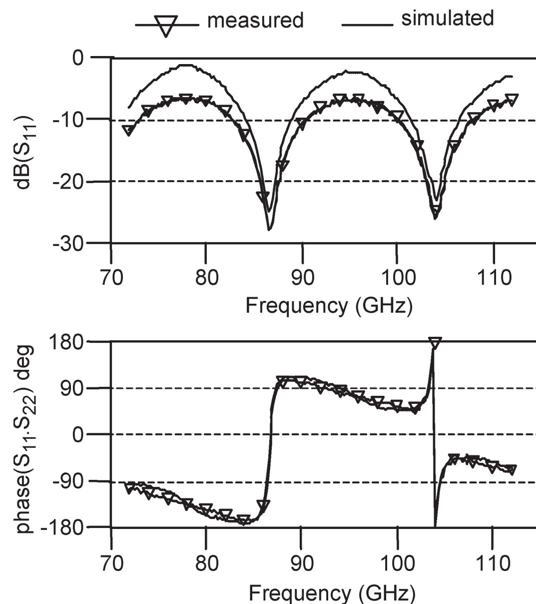

Fig. 7. Comparison between simulated and measured S_{11} parameter using an initial estimate of $\varepsilon_r' = 5.602$ from 3-D extraction.

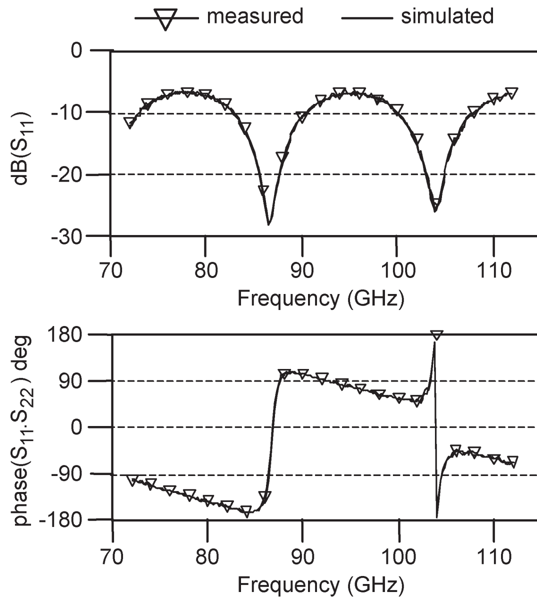

Fig. 8. Comparison between simulated and measured S_{11} parameter using an initial estimate of $\varepsilon'_r = 2.9$ from 3-D extraction.

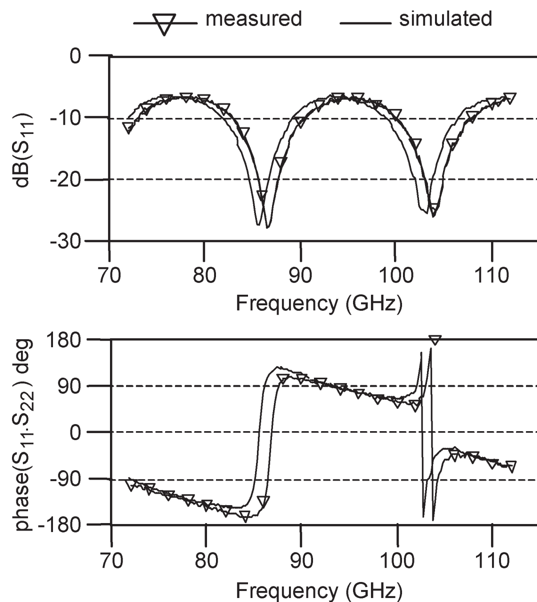

Fig. 9. Comparison between simulated and measured S_{11} parameter with $h = 5.16$ mm leading to a permittivity mean value $\varepsilon'_r = 2.885$ and $\varepsilon''_r = -0.00993$.

For the PVC slab, these values are $\varepsilon'_r = 2.931$ $(\sigma = 0.004)$ an d $\varepsilon''_r = -0.01002$ $(\sigma = 0.003)$.

IV. Experimental Results

Using the previously described calibration, measurement and optimization procedures, dielectric slabs and materials were characterized in the W-band. Table I, which gives the calculated mean values of ε'_r, ε''_r, and the loss tangent, summarizes the characterization results for various specimens. Some of these results are detailed and discussed in this section.

The foam polymethacrylimide (PMI—density: 71 kg/m^3) is found to be a very interesting material because of its lightness, its permittivity close to unity, and its low losses at very high frequencies. This material can be tooled to obtain 3-D objects and metallized to design microwave circuits such as antennas. From measurements of a 9.93-mm-thick foam slab, the extracted real and imaginary parts of the relative permittivity with frequency are depicted in Fig. 10. As shown, the relative permittivity of this material is approximately constant over the W-band. Thus, calculated mean values of ε'_r and ε''_r are, respectively, 1.069 and -0.003. The calculated loss tangent is 2.79 10^{-3}. This very low value demonstrates that the characterization of very low-loss materials can be achieved with the test bench as cavity techniques do. Moreover, this specific material is very interesting to validate the calibration procedure and the proposed extraction technique. Due to the permittivity of the dielectric slab close to unity, the reflection coefficients should be very low and, at frequencies for which the slab thickness is equal to $n\lambda_0/2$ (n is an integer), no reflection from the dielectric slab should be observed. These theoretical results are well confirmed by the S-parameter measurements as shown in Fig. 11 where only the comparison between the measured and simulated S_{11} parameter is depicted. Note that our free-space measurement setup is able to measure reflection coefficients as low as -50 dB.

This second example applies to alumina substrate, which is commonly used for the design of microwave circuits and in the millimeter wave range (very low losses at these high frequencies). A 635-μm-thick alumina slab is characterized, and the result of the extracted real part of the relative permittivity is depicted in Fig. 12. From the extracted permittivity over the W-band, an average value of $\varepsilon'_r = 8.83$ can be calculated. This result shows that the permittivity of alumina varies from the typical values observed below 20 GHz ($\varepsilon'_r = 9.5$ at 1 MHz depending on the alumina purity (96% for ADS-96R). The extraction of tan δ from the measurements is not efficient for this very thin and low-loss material as the values of ε''_r are widely spread. A value of tan δ lower than 10^{-3} is thus presumed.

The next example concerns the characterization of a low-loss plastic material (Rexolite 1422) used in lens antenna manufacturing for car collision avoidance radar at 77 GHz. The results are depicted in Fig. 13. As shown, the extracted real part of the Rexolite 1422 permittivity is constant with frequency over the W-band. The calculated mean values $\varepsilon'_r = 2.534$ and $\tan\delta = 1.3\,10^{-3}$ are very close to the manufacturer values $\varepsilon'_r = 2.53$ given from 1 MHz up to 500 GHz and $\tan\delta = 0.00066$ at 10 GHz. The loss tangent average is accurately determined using a 12.85-mm-thick plate as ε'_r and ε''_r are constant with frequency.

Besides the various substrates used to design microwave circuits, very different materials such as cement-based materials, polymers, liquids, paints, plywood, or fiberboard can be characterized. Wood-based nonhomogeneous high-loss materials were characterized, and the extraction leads to effective or equivalent values of the real and imaginary parts of the permittivity. The 18.3-mm-thick chipboard plate was first measured. The calculated mean value of ε'_r is 2.224, and the loss tangent is 0.0857. The second material is a 17.88-mm-thick plywood plate. The calculated mean value of ε'_r is 2.371, and the loss tangent is 0.0578.

TABLE I
PERMITTIVITY EXTRACTION OF VARIOUS MATERIALS IN THE W-BAND

Material/trade name	Manufacturer	ε_r'	ε_r''	tan δ
PVC (Polyvinyl Chloride)	Rohm & Haas	2.931	-0.029	0.01002
PMI Rohacell® HF	De Gussa	1.069	-0.003	0.0028
Alumina ADS-96R	Coors	8.85	-	$< 10^{-3}$
Rexolite 1422	-	2.534	-0.003	0.0013
Polyetherimide PEI	-	3.063	-0.023	0.0074
Polymer	-	2.665	-0.109	0.0407
Plywood	-	2.371	-0.137	0.0578
Chipboard	-	2.224	-0.191	0.0857

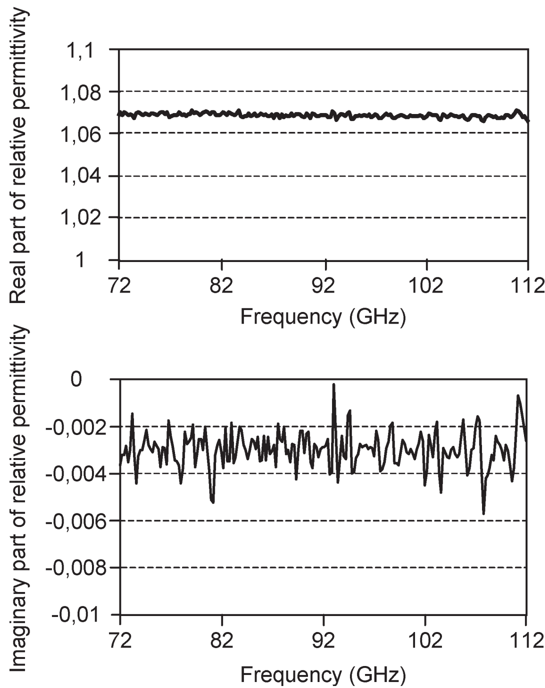

Fig. 10. Permittivity extraction of a PMI foam plate ($h = 9.93$ mm) over the extended W-band (72–112 GHz).

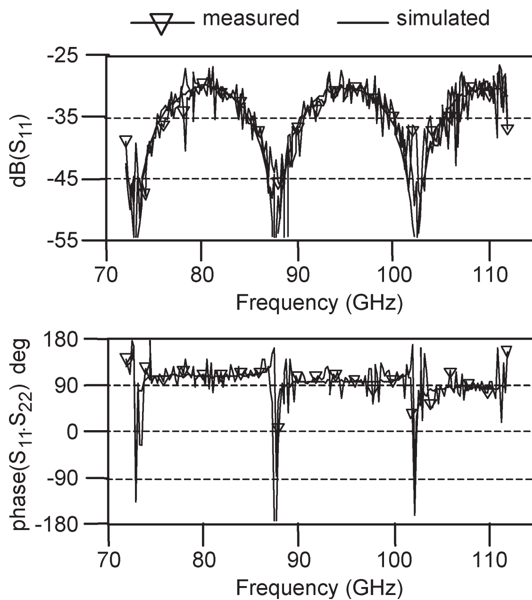

Fig. 11. Comparison between simulated and measured S_{11} parameter of a PMI foam plate ($h = 9.93$ mm).

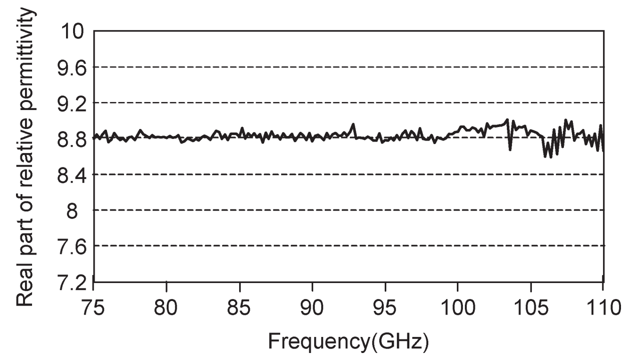

Fig. 12. Permittivity extraction of an alumina plate ($h = 635$ μm) over the W-band.

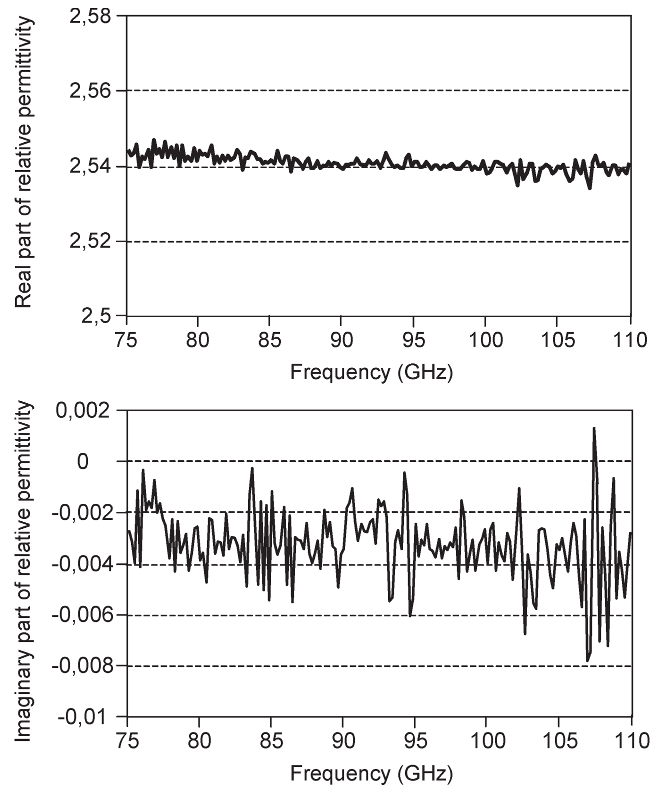

Fig. 13. Permittivity extraction of a Rexolite 1422 plate ($h = 12.85$ mm) over the W-band.

V. CONCLUSION

The new test bench described in this paper provides accurate free-space four S-parameter measurements of dielectric slabs without time gating. The Gaussian beam theory leads to specifications of the horn antenna in terms of paraxiality, which

makes calibration and measurements very accurate over the whole W-band. An efficient procedure for the extraction of the dielectric constant has been proposed, and the characterization of various materials is accurately achieved. Thus, the straightforward automation of the bench is possible with homogeneous materials. An extension to multilayer plate characterization is currently under study. In future work, this bench will be adapted to measure quasi-optical devices such as filters, polarizers, or active grids.

ACKNOWLEDGMENT

The authors would like to thank B. Deschamps (Agence Nationale des Fréquences, Brest, France), and R. Sauleau (Université de Rennes, France), for supplying dielectric slabs.

REFERENCES

[1] B. G. Helme, "Measurements of the microwave properties of materials," in *Proc. IEE Colloq. Ind. Uses Microwaves*, 1990, pp. 1–7.
[2] N. Williams, V. K. Varadan, D. Ghodgaonkar, and V. V. Varadan, "Measurement of transmission and reflection of conductive lossy polymers at millimeter-waves frequencies," *IEEE Trans. Electromagn. Compat.*, vol. 32, no. 3, pp. 236–240, Aug. 1990.
[3] J. Barker-Jarvis *et al.*, "Dielectric characterization of low-loss materials—A comparison of techniques," *IEEE Trans. Dielectr. Electr. Insul.*, vol. 5, no. 4, pp. 571–577, Aug. 1998.
[4] T. E. Talpey, "Optical methods for the measurement of complex dielectric and magnetic constants at centimeter and millimeter wavelengths," *IEEE Trans. Microw. Theory Tech.*, vol. MTT-2, no. 3, pp. 1–12, Sep. 1954.
[5] R. G. Nitsche, J. PreiBner, and E. M. Biebl, "A free-space technique for measuring the complex permittivity and permeability in the millimeter wave range," in *Proc. IEEE MTT-S Dig.*, Jun. 1994, vol. 3, pp. 1465–1468.
[6] G. L. Friedsam and E. M. Biebl, "A broadband free-space dielectric properties measurement system at millimeter wavelengths," *IEEE Trans. Instrum. Meas.*, vol. 46, no. 42, pp. 515–518, Apr. 1997.
[7] D. Thompson, R. E. Miles, and R. D. Polland, "Complex permittivity measurements using a quasi-optical multistate reflectometer," in *Proc. IEEE 6th Int. Conf. Terahertz Electron.*, Sep. 1998, pp. 163–165.
[8] R. D. Hollinger, K. A. Jose, A. Tellakulla, V. V. Varadan, and V. K. Varadan, "Microwave characterization of dielectric materials from 8 to 110 GHz using a free-space set-up," *Microw. Opt. Technol. Lett.*, vol. 26, no. 2, pp. 100–105, Jul. 2000.
[9] F. I. Shimabukuro *et al.*, "A quasi-optical method for measuring the complex permittivity of materials," *IEEE Trans. Microw. Theory Tech.*, vol. MTT-32, no. 7, pp. 659–665, Jul. 1984.
[10] M. N. Afsar, I. I. Tkachov, and K. N. Kocharyan, "A waveguide bridge/quasi-optical *W*-band spectrometer for dielectric measurement of absorbing materials," in *Infrared and Millimeter Waves Int. Conf. Dig.*, Sep. 2000, pp. 393–394.
[11] D. K. Ghodgaonkar, V. V. Varadan, and V. K. Varadan, "A free-space method for measurement of dielectric constants and loss tangents at microwave frequencies," *IEEE Trans. Instrum. Meas.*, vol. 37, no. 3, pp. 789–793, Jun. 1989.
[12] P. F. Goldsmith, "Quasi-optical techniques offer advantages at millimeter frequencies," *Microw. Syst. News*, vol. 13, no. 134, pp. 65–84, Dec. 1983.
[13] L. E. R. Petersson and G. S. Smith, "An estimate of the error caused by the plane-wave approximation in free-space dielectric measurement systems," *IEEE Trans. Antennas Propag.*, vol. 50, no. 6, pp. 878–887, Jun. 2002.
[14] N. Grignon *et al.*, "Material characterization using a quasi-optical measurement system," *IEEE Trans. Instrum. Meas.*, vol. 52, no. 2, pp. 333–336, Apr. 2003.
[15] P. Goy and M. Gross, "Free-space vector transmission-reflection from 18 to 760 GHz," in *Proc. 24th EuMC*, Oct. 1994, pp. 1973–1978.
[16] R. J. Wylde, "Millimeter-wave Gaussian beam-mode optics and corrugated feed horns," *Proc. Inst. Electr. Eng.*, vol. 131, no. 4, pp. 258–262, Aug. 1984.
[17] P. S. Kildal, "Gaussian beam model for aperture-controlled and flareangle-controlled corrugated horn antennas," *Proc. Inst. Electr. Eng.*, vol. 135, no. 4, pp. 237–240, Aug. 1988.
[18] S. Nemoto, "Nonparaxial Gaussian beams," *Appl. Opt.*, vol. 29, no. 13, pp. 1940–1946, May 1990.
[19] M. LeGoff, J. L. Le Bras, B. Deschamps, D. Bourreau, and A. Péden, "Ka band quasi optical test bench using focusing horns," in *Proc. 29th Eur. Microw. Conf.*, Munich, Germany, Oct. 1999, pp. 240–243.
[20] G. F. Engen and C. A. Hoer, "Thru-reflect-line: An improved technique for calibrating the dual six port automatic network analyzer," *IEEE Trans. Microw. Theory Tech.*, vol. MTT-27, no. 12, pp. 987–993, Dec. 1979.
[21] C. A. Balanis, *Advanced Engineering Electromagnetics*. Hoboken, NJ: Wiley, 1989.

Daniel Bourreau was born in Voultegon, France, in 1959. He received the Ph.D. degree in electronics from the University of Lille, Lille, France, in 1989.

He joined the Laboratoire d'Electronique et de Systèmes des Télécommunications de Bretagne, Ecole Nationale Supérieure des Télécommunications, Brest, France, in 1989. He is currently an Associate Professor, and his research interests include microwave and millimeter-wave oscillators and power generation using combining and quasi-optical techniques.

Alain Péden received the Diplôme d'Etudes Supérieures Spécialisées degree from the University of Limoges, Limoges, France, in 1985 and the Ph.D. degree in electronics from the Ecole Nationale Supérieure des Télécommunications, Brest, France, in 1991.

From 1986 to 1988, he was a monolithic microwave integrated circuit Designer with Thomson Composants Microondes. He joined the Laboratory of Electronics and Systems for Telecommunications (LEST), Ecole Nationale Supérieure des Télécommunications, Brest, in 1989. He is currently an Associate Professor, and his research activities are in the field of microwave and millimeter-wave power amplifier design. He is mainly involved with the large signal characterization of transistors and nonlinear devices and applications to amplifier design using power combining and quasi-optical techniques.

Sandrick Le Maguer received the Electrical Engineering Diploma from the Ecole Superieur d'Ingenieur en Genie Electrique, Rouen, France, in 1993 and the Ph.D. degree in electronics from the Ecole Nationale Supérieure des Télécommunications, Brest, France, in 1998.

He joined the Laboratoire d'Electronique et de Systèmes des Télécommunications de Bretagne, Ecole Nationale Supérieure des Télécommunications, Brest, in 1995. Since 2000, he has been an Associate Professor. His research interests include time-domain numerical modeling and its implementation to analyze microwave and millimeter-wave circuits and electromagnetic compatibility. His recent research topics are focused on new high-speed algorithms with emphasis on cognitive sciences potentialities.